Available online at www.sciencedirect.com
ScienceDirect
Journal of Computational Physics 220 (2007) 900–914
JOURNAL OF COMPUTATIONAL PHYSICS
www.elsevier.com/locate/jcp

Fourth order accurate evaluation of integrals in potential theory on exterior 3D regions

Anita Mayo [a,1], Anne Greenbaum [b,*,2]

[a] *Baruch College, CUNY, New York, NY, USA*
[b] *Department of Mathematics, University of Washington, Box 354350, Seattle, WA 98195, USA*

Received 18 July 2005; received in revised form 25 May 2006; accepted 29 May 2006
Available online 17 August 2006

Abstract

We present two methods for the rapid, high order accurate evaluation of integrals in potential theory on general, unbounded 3D regions. Our methods allow for direct calculation of derivatives of the integrals as well. One of the methods uses a fourth order compact stencil, and the other uses a nonstandard variant of Richardson extrapolation. Both methods involve calculation of discontinuities in high order derivatives of the integrals across the boundary of the integration region. The extrapolation method, in addition, involves correction for the discontinuities in truncation error. The number of operations required for the methods is essentially equal to twice the number of operations needed to solve Poisson's equation on a regular grid. Both methods avoid problems associated with using quadrature methods to evaluate integrals with singular kernels. Numerical results are presented for experiments on a variety of geometries in free space.

Keywords: Potential theory; Integrals and their derivatives; High order; Unbounded 3D regions

1. Introduction

In this paper we develop fast, fourth order accurate methods for evaluating volume and surface integrals in potential theory on general, unbounded three-dimensional regions. The methods are mesh based, and are generalizations of our previous work (see [15,30–37]).

Integral equation methods are often used for solving elliptic boundary value problems, especially on exterior regions. In particular, they are frequently used for problems in electromagnetics [2,21,23,25,29], aerodynamics [20], acoustics [6] and fluid dynamics [40]. The solution of such equations has been researched extensively, and many effective methods are available. Among these are methods based on the fast multipole method [11,14,17,18,42,43], wavelets [1], singular value decompositions [4,5], and other sparse representations.

* Corresponding author. Tel.: +1 206 543 1175.
E-mail address: greenbau@math.washington.edu (A. Greenbaum).
[1] This work was supported by PSC-CUNY Grant 60094-3435.
[2] This work was supported by DOE Grant DEFG0288ER25053.

0021-9991/$ - see front matter © 2006 Elsevier Inc. All rights reserved.
doi:10.1016/j.jcp.2006.05.042

Despite these advances, difficulties are often encountered when integral equation methods are used to solve realistic problems, especially nonhomogeneous ones where the equations therefore contain volume integrals. First, it is expensive to compute the solution at many points by evaluating an integral. While one can evaluate volume integrals in two dimensions using only $O(n^2)$ operations via the fast multipole method [11,16], the method has not proven practical in 3D because the constants are so large. If one uses straightforward quadrature methods a total of $O(n^6)$ operations are needed to evaluate a volume integral in a three-dimensional region of $O(n^3)$ points since evaluating each integral requires $O(n^3)$ operations. Also, because the kernels have $O\left(\frac{1}{r}\right)$ singularities, standard quadrature methods are ineffective at nearby points, and implementations must have greater complexity.

In prior work we developed methods which overcome these difficulties. In these methods the integral is evaluated by quadrature only at points at the edge of a regular region in which the irregular region is embedded. Using these techniques we obtain full accuracy at mesh points near the boundary of the irregular region without interpolation, and we can compute the derivatives of the integral directly with little loss of accuracy if the boundary of the region is sufficiently smooth. This is particularly important in applications since usually only derivatives of the integral are needed.

To be specific, we have solved Poisson's [30,31,34] and the biharmonic equations [33], and the Navier Stokes equations at low Reynolds number in two dimensions [36]. In addition, we have solved an exterior interface problem in magnetic recording, used the method to develop a rapid method of conformal mapping [32], and solved problems in fluid dynamics with immersed interfaces [28,37]. We have also parallelized the method in two and three dimensions [15,31].

In these second order accurate methods we embed the irregular region in a rectangular region with a regular grid. We approximate the integral U by approximating its second order accurate discrete Laplacian, Δ_h, at all points of the grid, and then inverting the discrete Laplacian. To compute an approximation to $\Delta_h U$ we use known values of the Laplacian of U at points inside and outside the integration region, and discontinuities in the derivatives of the integral at the boundary of the integration region.

In this paper we present fourth order accurate versions of our methods. One uses a fourth order compact 19 point stencil. The use of this stencil required development of easily evaluated formulas for the discontinuities in higher order derivatives of the integrals. Because we were solving exterior problems we also needed to use a fourth order accurate discrete free space Green's function.

The other fourth order accurate method is an extrapolation method. In this method we compute two approximations to the integrals using two different meshes, and then combine them to obtain a fourth order accurate solution. Neither of the two original approximations is the standard second order accurate approximation, although the computation of both requires the inversion of the usual second order discrete Laplacian. The method relies on the fact that when one uses a second order discrete Laplacian in our method, the truncation errors are the same as they would be if the integrals were smooth across the irregular boundary. However, because the truncation errors are discontinuous, the usual linear combination of two approximations obtained will not be fourth order accurate. Instead, we must first correct for the truncation error discontinuities before inverting the discrete Laplacians and combining the results. Our extrapolation method can also be used to obtain a more accurate solution on just part of the computational domain. Richardson extrapolation is also useful in obtaining error estimates. Furthermore, we can continue using Richardson extrapolation to obtain sixth order accurate approximations to the integrals. We have also found that since one can invert the 7 point second order stencil more rapidly than the 19 point fourth order accurate stencil, this method is somewhat faster than the method which uses the fourth order discretization. This is because using FACR algorithms one can invert the 7 point stencil with $O(n^3 \log\log n)$ operations. The fast Fourier methods used to invert the fourth order 19 point stencil require $O(n^3 \log n)$ operations. However, although both methods are fourth order accurate, in practice we have found the extrapolation method to be slightly less accurate.

In contrast to our earlier work the methods presented here are also effective on exterior regions. When using finite difference methods on exterior problems boundary values at the edge of the grid are needed. Although they can be obtained by quadrature, in three dimensions this requires $O(n^5)$ operations. Another possibility is an algorithm developed by Hockney where one doubles the mesh in each direction, and then uses Fourier methods. Unfortunately, this requires one to use twice the storage needed for the original problem. In an alternate procedure developed by James [22] one only needs to double the mesh on the surface of the embedding

region. The cost of this method on a uniform grid is the same as the cost of inverting the discrete Laplacian on that mesh, and the extra storage is minimal. This method also requires a free space discrete Green's function. For calculations in our extrapolation method we have used a free space discrete Green's function developed by Burkhart [8], and for calculations with fourth order accurate stencils we have used one proposed by James [22].

Among the primary advantages of our methods is that they do not require mesh generation in the interior of the irregular region, often the most difficult part of the calculation [44].

We note that our methods for evaluating integrals are essentially methods for solving an elliptic differential equation with discontinuous coefficients. Of course, finite element methods are most often used for solving such equations on general regions. However, mesh generation can be quite expensive for large 3D problems, and the most rapid means of solving the discretized differential equations normally require a regular mesh. Although multigrid and domain decomposition methods can have optimal complexity, they require the use of multilevel methods. These in turn require a hierarchy of coarse grids, which can be difficult to obtain in complicated regions.

Among the most effective methods for solving elliptic problems in complex geometries are those based on regular grids. The earliest of these are known as capacitance matrix methods [10]. In particular, methods developed by Widlund and coworkers [41] also use the embedding of the irregular region in a rectangular region, and refer to an integral equation formulation. In their methods standard finite difference equations are modified when a stencil crosses the boundary. The resulting matrix, known as a capacitance matrix, can be written as the sum of the identity and an approximation to a compact operator on the boundary. They formulate the problem so that the matrices are approximations to Fredholm integral equations of the second kind, which they solve iteratively. Because the spectrum tends to be clustered, the convergence can be quite rapid. However, we note that capacitance methods cannot take advantage of optimal methods of solving integral equations, and instead require a variable number of solutions of the regular grid problem. They also do not allow direct computation of derivatives, nor do they easily allow development of fourth order accurate versions for highly irregular regions.

Another important technique is the immersed boundary method developed by Peskin and McQueen [39]. It was originally designed as part of a method for solving the unsteady Navier Stokes equations when there is an infinitely thin interface contained in the fluid upon which there is a force. In this method the interface is modeled as a set of discrete delta functions which are spread to the mesh. If the interface is not smoothed it is only first order accurate, and as in all particle mesh methods the results obtained are somewhat embedding dependent. It has been used to solve a wide variety of problems in computational biology, including aquatic locomotion [13].

The immersed interface method [26] is a second order accurate extension of the immersed boundary method. It uses essentially the same method as [33] for problems with constant coefficients if the discontinuities in the function and its derivatives across the interface are known. However, variants of it have been developed for solving problems with nonconstant coefficients, as well as for solving Neumann and Dirichlet problems. In those cases the stencil is modified at points near the boundary to account for the jump conditions. The method then results in matrices to which standard fast methods are not applicable, and variable numbers of regular grid solves are required. It has been successfully applied to many problems including the Navier Stokes problem [27].

Beale and Lai [3] have proven that in both [33] and the immersed interface method the solution can be computed to $O(h^2)$ accuracy uniformly, and the gradient can be computed to $O(h^2\log(1/h))$ accuracy even if the truncation error is $O(h)$ at the interface, as long as it is $O(h^2)$ elsewhere.

The stencils are also modified in the Cartesian finite volume methods [23] developed by Johansen and Colella. They have solved variable coefficient Poisson problems in the presence of an irregular interface on which Dirichlet boundary conditions were imposed. Their method results in nonsymmetric discretization matrices, and is combined with multigrid and adaptive mesh refinement techniques.

More recently Zhou et al. [46] introduced a high order interface scheme, the matched interface and boundary method (MIB) for solving elliptic equations with discontinuous coefficients and singular sources on Cartesian grids. In this method the jump conditions are disassociated from the discretization by repeated enforcement of the lowest order jump conditions.

Another new method is the second or fourth order accurate boundary capturing method due to Gibou and Fedkiw [12]. It can be used for solving Dirichlet problems for the variable coefficient Poisson equation on general regions, and results in symmetric positive definite matrices with diagonally modified stencils and additional terms on the right-hand side. In this method, as in Johansen and Colella's method, one cannot use standard fast methods for solving difference equations on rectangular domains such as those based on the FFT. Instead one must use iterative techniques.

We also note that, to our knowledge, none of the above methods have been used for the fourth order accurate evaluation of volume integrals in free space.

The organization of this paper is as follows. In Section 2 we show how to compute second order accurate approximations to volume integrals, in Section 3 we present the method which uses the 19 point fourth order stencil, and in Section 4 we present our extrapolation method. In Section 5 we discuss boundary conditions, and in Section 6 we discuss operation counts and extensions. In Section 7 we provide numerical results.

2. Second order accurate evaluation of volume integrals

We first show how to compute a second order accurate approximation to a volume integral whose kernel is the free space Green's function for the Poisson equation:

$$U(x,y,z) = \frac{1}{4\pi}\int\int_D\int \frac{1}{r(x,y,z,x',y',z')} f(x',y',z')\mathrm{d}x'\mathrm{d}y'\mathrm{d}z', \tag{2.1}$$

where $r(x,y,z,x',y',z') = \sqrt{(x-x')^2+(y-y')^2+(z-z')^2}$.

We embed the region of integration D in a larger rectangular region R with mesh widths (h_x,h_y,h_z), and use the standard 7 point approximation to the Laplacian:

$$(\Delta_h^7 U)_{i,j,k} = \frac{U_{i+1,j,k}+U_{i-1,j,k}-2U_{i,j,k}}{h_x^2} + \frac{U_{i,j+1,k}+U_{i,j-1,k}-2U_{i,j,k}}{h_y^2} + \frac{U_{i,j,k+1}+U_{i,j,k-1}-2U_{i,j,k}}{h_z^2}.$$

To approximate U we compute an approximation to $\Delta_h^7 U$ at all points of R, and then apply a Poisson solver. Since

$$\Delta U = f \text{ in } D,\ \Delta U = 0 \text{ outside } D, \tag{2.2}$$

at mesh points (i,j,k) inside D that have all their neighbors in D, we set $(\Delta_h^7 U)_{ijk} = f_{ijk}$, and at outside points whose neighbors are also outside D we set $(\Delta_h^7 U)_{ijk} = 0$.

We cannot use either formula at points near ∂D because the derivatives U of second and higher order are not continuous there.

Let B be the set of irregular mesh points, that is the set of points which have one or more of their neighbors on the other side of ∂D. At points of B an approximation to $\Delta_h^7 U$ can be expressed in terms of the discontinuities in U and its derivatives in the coordinate directions at the boundary of D.

Suppose the boundary surface is locally given by $x(s,t)$, $y(s,t)$, $z(s,t)$. where s and t are two real parameters.

Since an integral of the form (2.1) and its normal derivative U_n are continuous across ∂D [24], the components of the gradient are also continuous.

By (2.2) there must be discontinuities in the second derivatives of U.

To determine discontinuities in the six second derivatives of U we differentiate (2.2) in the normal and tangential directions, and use the discontinuity in the Laplacian. This gives a system of six equations we can solve for the discontinuities in the six second derivatives of U in the coordinate directions. (The coefficients of the system depend on the functions $x(s,t)$, $y(s,t)$, $z(s,t)$ and their derivatives [33].)

These discontinuities are used to determine the discrete Laplacian of U at the irregular mesh points B.

Suppose, for example, that a mesh point p is in D, but the neighboring mesh point to the right, p_{E}, is not. Let p^* be the point on the line between p and p_{E} which intersects ∂D, let h_1 be the distance between p and p^*, and let $h_2 = h - h_1$.

We can derive the following expression for $U(p_{\mathrm{E}}) - U(p)$ by manipulating the Taylor series at p and p_{E} both evaluated at p^*. For details see [33].

$$U(p_E) - U(p) = [U(p^*)] + h_2[U_x(p^*)] + \frac{1}{2}h_2^2[U_{xx}(p^*)] + \frac{1}{6}h_2^3[U_{xxx}(p^*)] + \frac{1}{24}h_2^4[U_{xxxx}(p^*)] + hU_x(p) + \frac{h^2}{2}U_{xx}(p) + \frac{h^3}{6}U_{xxx}(p) + \frac{h^4}{24}U_{xxxx}(p) + O(h^5). \tag{2.3}$$

Here $[g]$ denotes the discontinuity in a function g at a point on ∂D. The first four terms depend on the discontinuities in U and in its x derivatives at the boundary, and the other terms are the usual Taylor series terms. Therefore, the right-hand side of (2.3) is a sum of terms we can evaluate in terms of the discontinuities in U and its derivatives, and terms we would have if there were no boundary between p and p_E.

We obtain the same type of expressions for the differences between the value of U at p and at its other neighbors, except that there will not be any boundary discontinuity terms unless ∂D passes between p and that neighbor. Therefore, at any of the irregular points. we can compute an approximation to the 7 point discrete Laplacian of U, which is just the scaled sum of the differences between the values of U at that point and at its neighbors. More precisely, for mesh points $(i,j,k) \in B$ we define the mesh function m^h_{ijk} to be the value of the extra terms in the discrete Laplacian we get by our procedure using f and its derivatives.

We define U_h to be the solution of the following equations:

$$\Delta_h^7 U_h = \begin{cases} f_{ijk} & (i,j,k) \in D - B, \\ f_{ijk} + m^h_{ijk} & (i,j,k) \in B \cap D, \\ m^h_{ijk} & (i,j,k) \in B \cap D^c, \\ 0 & (i,j,k) \in R - D - B. \end{cases} \tag{2.4}$$

If the values of $m^h_{i,j,k}$ are second order accurate, then by applying a second order accurate Poisson solver the function U_h we obtain is a second order accurate approximation to U. See [33,34].

3. Fourth order accurate stencil

We have computed fourth order accurate approximations to integrals of the form (2.1) by using a fourth order accurate stencil. Specifically, we have used the 19 point stencil

$$\Delta_h^{19} U = \frac{2}{3}\Delta_h^7 U + \frac{1}{6}\Delta_h^{13} U = \Delta U + \frac{1}{12}\Delta\Delta U,$$

where

$$\begin{aligned}(\Delta_h^{13} U)_{i,j,k} = {} & (U_{i+1,j+1,k} + U_{i-1,j+1,k} + U_{i+1,j-1,k} + U_{i+1,j-1,k} - 4U_{i,j,k})\left(\frac{1}{h_x^2} + \frac{1}{h_y^2}\right) \\ & + (U_{i+1,j,k+1} + U_{i-1,j,k+1} + U_{i+1,j,k-1} + U_{i+1,j,k-1} - 4U_{i,j,k})\left(\frac{1}{h_x^2} + \frac{1}{h_z^2}\right) \\ & + (U_{i,j+1,k+1} + U_{i,j-1,k+1} + U_{i,j+1,k-1} + U_{i,j-1,k-1} - 4U_{i,j,k})\left(\frac{1}{h_y^2} + \frac{1}{h_z^2}\right).\end{aligned}$$

To obtain a fourth order accurate approximation to an integral U, we first compute a fourth order accurate approximation to $\Delta_h^{19} U$. To do this we need to find differences in the values of U in the oblique directions as well as the coordinate directions. These differences can be expressed as the sum of the usual Taylor series terms and the discontinuities in the derivatives of U in the oblique directions. If the approximation to $\Delta_h^{19} U$ is to be third order accurate we also need to retain more terms in the series expansions.

For example, suppose the point $p = (x_i, y_j, z_k)$ is in D and the point $p_{NE} = (x_{i+1}, y_{j+1}, z_k)$ is not. Denote by $p^* = (x^*, y^*, z^*)$ the point where the line between p and p_{NE} intersects ∂D. We let $h_{1x} = x^* - x_i$, $h_{1y} = y^* - y_j$, $h_{2x} = h_x - h_{1x}$ and $h_{2y} = h_y - h_{1y}$.

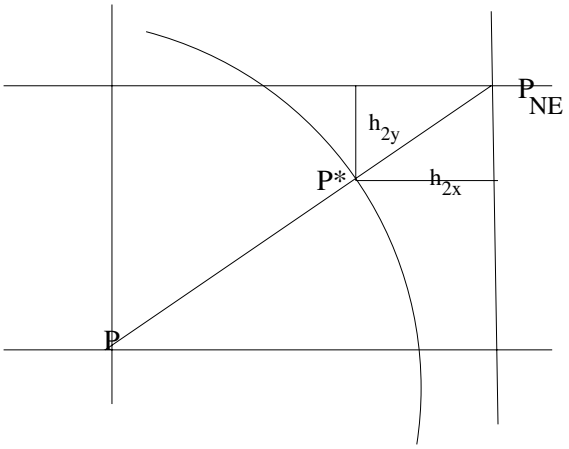

Instead of an expansion of the form (2.3) straightforward Taylor series manipulations in both the x and y directions show that the difference $U_{PE} - U_P$ is equal to the sum of the discontinuity terms

$$
\begin{aligned}
&- h_{2x}[U_x(p^*)] - h_{2y}[U_y(p^*)] - \frac{h_{2x}^2}{2}[U_{xx}(p^*)] - h_{2x}h_{2y}[U_{xy}(p^*)] - \frac{h_{2y}^2}{2}[U_{yy}(p^*)] - \frac{h_{2x}^3}{6}[U_{xxx}(p^*)] \\
&- \frac{h_{2x}^2 h_{2y}}{2}[U_{xxy}(p^*)] - \frac{h_{2x}h_{2y}^2}{2}U_{xyy}(p^*) - \frac{h_{2y}^3}{6}[U_{yyy}(p^*)]\frac{h_{2x}^4}{24}[U_{xxxx}(p^*)] - \frac{h_{2x}^3 h_{2y}}{6}[U_{xxxy}(p^*)] \\
&- \frac{h_{2x}^2 h_{2y}^2}{4}[U_{xxyy}(p^*)] - \frac{h_{2x}h_{2y}^2}{6}[U_{xyyy}(p^*)] - \frac{h_{2y}^4}{24}[U_{yyyy}(p^*)]
\end{aligned} \tag{3.1}
$$

and the usual Taylor series terms.

The terms involving lower order discontinuities in derivatives of U at p^* can be determined using the method detailed in Section 2. Now, however, we also need to compute discontinuities in higher order derivatives. To compute the discontinuities in the 10 third order derivatives, U_{xxx}, U_{xxy}, $U_{xxz}U_{xyy}$, U_{xyz}, U_{xzz}, U_{yyy}, U_{yyz}, U_{xzz}, and U_{zzz} we use the 10 equations

$$
\begin{aligned}
&[U_{sss}] = [U_{sst}] = [U_{stt}] = [U_{ttt}] = 0, \\
&[U_{nss}] = [U_{nst}] = [U_{ntt}] = 0, \\
&[(\Delta U)_s] = f_s, [(\Delta U)_t] = f_t [(\Delta U)_n] = f_n.
\end{aligned}
$$

Discontinuities in higher order derivatives are computed similarly.

Once we have formed a fourth order accurate approximation to $\Delta_h^{19}U$ we need to invert the operator Δ_h^{19}. We have chosen to perform the calculation using the Fast Sine Transform. That is, since we are using Dirichlet boundary conditions (see Section 5) we first calculate the three-dimensional Fast Sine Transform of our approximation to $\Delta_h^{19}U$. Then we divide the result by the symbol of the operator Δ_h^{19}. Finally, we apply the three-dimensional inverse Fast Sine Transform.

Since the discrete operator $(\Delta_h^{19})^{-1}$ is bounded, it follows that the solution obtained, U_h, will be a fourth order accurate approximation to U.

4. Extrapolation method

In the method of Richardson extrapolation one computes two approximations to the solution of a problem using two different meshes. Then one forms a linear combination of these approximations so that the leading terms in the truncation errors cancel. One thereby obtains a higher order accurate approximation.

If the original approximation method is second order accurate, then one generally computes a solution V_h with a mesh of some width h, and another one, V_{2h} using a mesh twice as wide. The function $\frac{4V_h - V_{2h}}{3}$ is then a

fourth order accurate approximation to the solution of the problem V. The procedure relies on the existence of an expansion of the form $V = V_h + h^2 E + \mathrm{O}(h^4)$ where the function E is independent of h.

Because of the discontinuities in the derivatives of the truncation error, we will not obtain a fourth order accurate solution if we use the second order accurate method presented in Section 2. However, it turns out that we can easily correct for these discontinuities.

First note that if we include boundary discontinuities in higher order derivatives of the integral U when we approximate its 7 point discrete Laplacian, the truncation error will contain the usual fourth order derivatives of the integral, as if there were no discontinuities in the derivatives U. That is,

$$\Delta_h^7(U - U_h) = \frac{h_x^2}{12} U_{xxxx} + \frac{h_y^2}{12} U_{yyyy} + \frac{h_z^2}{12} U_{zzzz} + \mathrm{O}(h^4) \tag{4.1}$$

As when the solution of a Poisson problem is continuous, we consider the functions whose Laplacians are equal to the leading terms in the truncation error. Specifically, we let $E_x(x,y,z)$, $E_y(x,y,z)$ and $E_z(x,y,z)$ be the (piecewise differentiable) functions whose Laplacians are equal to the coefficients of the terms of order h^2 on the right-hand side of (3.1), and which are continuous in the tangential and normal directions across ∂D:

$$\begin{aligned}
&\Delta E_x(x,y,z) = \frac{U_{xxxx}}{12},\\
&\Delta E_y(x,y,z) = \frac{U_{yyyy}}{12},\\
&\Delta E_z(x,y,z) = \frac{U_{zzzz}}{12},\\
&E_x(x,y,z), E_y(x,y,z), E_z(x,y,z),\\
&E_{xn}(x,y,z), E_{yn}(x,y,z), E_{zn}(x,y,z) \text{ continuous across } \partial D.
\end{aligned} \tag{4.2}$$

Because the fourth derivatives of $U(x,y,z)$ are not continuous across ∂D, the functions E_x, E_y, and E_z will have discontinuities in their second derivatives there. However, these discontinuities can be computed in terms of the discontinuities in the fourth derivatives of $U(x,y,z)$ using the method described in Section 2.

For given mesh width $h = (h_x, h_y, h_z)$ let e_x^h, e_y^h and let e_z^h denote the extra terms in the discrete Laplacians of E_x, E_y, and E_z that arise because of these discontinuities:

$$\begin{aligned}
(\Delta_h^7 E_x)_{i,j,k} &= \frac{U_{xxxx}}{12} + e_x^h(i,j,k) + \mathrm{O}(h^2),\\
(\Delta_h^7 E_y)_{i,j,k} &= \frac{U_{yyyy}}{12} + e_y^h(i,j,k) + \mathrm{O}(h^2),\\
(\Delta_h^7 E_z)_{i,j,k} &= \frac{U_{zzzz}}{12} + e_z^h(i,j,k) + \mathrm{O}(h^2).
\end{aligned} \tag{4.3}$$

The above equations allow us to correct for truncation error discontinuities. That is, instead of computing an approximation to the integral $U(x,y,z)$, for given h_x, h_y, h_z we compute an approximation to the function $\widetilde{U} = U - (h_x)^2 E_x - (h_y)^2 E_y - (h_z)^2 E_z$. Thus, instead of solving (2.4) we find the mesh function $\widetilde{U}_h$ such that

$$\Delta_h^7 \widetilde{U} = m_{i,j,k}^h + f_{i,j,k}^h - h_x^2 e_x^h(i,j,k) - h_y^2 e_y^h(i,j,k) - h_z^2 e_z^h(i,j,k). \tag{4.4}$$

We also recall that

$$\Delta_h^7 U = m_{i,j,k}^h + f_{i,j,k}^h + \frac{1}{12}(h_x^2 U_{xxxx} + h_y^2 U_{yyyy} + h_z^2 U_{zzzz}(i,j,k)) + \mathrm{O}(h_x^4; h_y^4; h_z^4). \tag{4.5}$$

Subtracting (4.4) from (4.5) and using (4.3) we see that

$$\Delta_h^7 U = \Delta_h^7(\widetilde{U}_h + h_x^2 E_x + h_y^2 E_y + h_z^2 E_z) + \mathrm{O}(h_x^4; h_y^4; h_z^4).$$

Since $(\Delta_h^7)^{-1}$ is a bounded linear operator it follows that

$$U = \widetilde{U}_h + h_x^2 E_x + h_y^2 E_y + h_z^2 E_z + \mathrm{O}(h_x^4; h_y^4; h_z^4). \tag{4.6}$$

Once we have computed an approximation $\widetilde{U}_h$ using a mesh of width $h = h_x$, h_y, h_z we double the mesh width in each direction and compute another approximation $\widetilde{U}_{2h}$ using the above procedure. The mesh function $\widetilde{U}_{2h}$ satisfies the equation

$$U = \widetilde{U}_{2h} + 4h_x^2 E_x + 4h_y^2 E_y + 4h_z^2 E_z + \mathrm{O}(h_x^4; h_y^4; h_z^4). \tag{4.7}$$

Multiplying (4.6) by 4 and subtracting (4.7) we see that the linear combination $\frac{4\widetilde{U}_h - \widetilde{U}_{2h}}{3}$ is a fourth order accurate approximation to U.

This assumes that correct boundary conditions have been imposed at the edge of the computational region. In the next section we show to impose these conditions.

5. Boundary conditions

In order to evaluate potential integrals using either of the fourth order accurate methods presented we need to prescribe accurate free space boundary values. In essence, we do this using a procedure suggested by James [22].

We first show how we can do this when we are using the fourth order accurate stencil. We start by using the method of Section 3 to find a mesh function ϕ_h whose 19 point discrete Laplacian is the same as that of the integral U, but which has zero Dirichlet boundary conditions at points in ∂R. After forming a fourth order accurate approximation to the discrete Laplacian of U at points inside R, we use a triple Fast Sine Transform [20] to invert it, although any other method could be used.

Next, setting the potential ϕ_h equal to zero at points outside R, we apply the fourth order discrete Laplace operator at points adjacent to the boundary points of R to determine what physicists call the "screening charge". That is, at points inside R which are one mesh width away from ∂R we form $q = \Delta_h^{19}\phi_h$.

Following this, we calculate the correction potential ψ_h due to the screening charges. The function ψ_h is the convolution of the screening charges with the fourth order accurate free space discrete Green's function.

The approximation potential is the difference between the two mesh functions ϕ_h and ψ_h: $U_h = \phi_h - \psi_h$. The procedure of computing screening charges and convolving them with a discrete free space Green's function in order to solve Poisson's equation in free space was first used by Von Hagenow and Lackner [45] and is discussed in Hockney and Eastwood [21].

When we use the extrapolation method the way free space boundary conditions are imposed is essentially the same. We begin by computing the mesh function ϕ_{1h} which is zero at the edge of the computational region R and whose 7 point discrete Laplacian is the same as that of the function $\widetilde{U}$. We do this using the procedure described in Section 4. That is, after forming the discrete Laplacian of $\widetilde{U}$ we solve (4.4) to find ϕ_{1h}, which involves inverting the 7 point discrete Laplacian. In our experiments we used the FACR algorithm from FISHPAK which combines the FFT with odd even reduction. We note that FACR algorithms exist for inverting the 19 point stencil, but they are not as effective.

Then we determine the screening charges due to ϕ_{1h}, i.e. after extending ϕ_{1h} by zero, we compute the 7 point discrete Laplacian at points in R less than one mesh width from ∂R. These screening charges are then convolved with the discrete free space Green's function for the 7 point Laplacian on the region R to obtain the correction potential, ψ_{1h}. We set $\widetilde{U}_{1h} = \phi_{1h} - \psi_{1h}$.

We then repeat this procedure using a mesh twice as wide, i.e. we solve for a mesh function ϕ_{2h}, and then compute the screening charge due to this function. Then we convolve the new screening charges with the discrete Green's function for the second order discrete Laplacian on the coarser mesh to obtain the correction potential ψ_{2h}. The mesh function ψ_{2h} is subtracted from ϕ_{2h} to obtain $\widetilde{U}_{2h}$.

Finally, we form our approximation $\frac{4U_{1h} - U_{2h}}{3}$.

The above methods of calculation require the second or fourth order accurate discrete free space Green's functions.

The solution $g(i,j,k)$ of a discrete equation

$$\Delta_h g(i,j,k) = \delta(i,j,k),$$

where Δ_h is any discrete Laplacian on a fixed mesh and $\delta(i,j,k)$ is a discrete Dirac delta function is known as a discrete Green's function. If, in addition, $g(i,j,k) = K(1/r + s(i,j,k))$ for constant K and mesh function $s(i,j,k)$

that goes to zero faster than $1/r$ then $g(i,j,k)$ is a discrete free space Green's function [9,22]. In two dimensions exact formulas for the free space discrete Green's function corresponding to both the second and fourth order accurate discrete Laplacians were given by Buneman [7,8], and are easy to compute.

In three dimensions no exact formulas are known. Often people solve problems on exterior regions merely by using a large computational grid and imposing zero Dirichlet conditions at the edge of the grid. Since it allows us to use a smaller computational region we have chosen instead to use asymptotic expansion methods to determine values of the free space discrete Green's functions at the edge of the embedding region R, and determine values inside R by solving the second or fourth order discrete Poisson equation with an unit source at the origin. This procedure is common [9,20,22]. In practice, since the Green's function is symmetric, we only need to know its value on a mesh which is the size of R.

To determine boundary conditions for the 7 point second order discrete Green's function we used the asymptotic expansion developed by Burkhart [9]. His expansion is valid for all orders, but we only use terms of order up to $O(\frac{1}{r^9})$.

For finding the boundary values of the discrete Green's function for the 19 point fourth order stencil we used the asymptotic expansion proposed by James [22].

We note that, as Burkhart has suggested, if the embedding region R is too small, the asymptotic expansion may not be accurate enough on its boundary. In that case one can start with a larger embedding region and partially solve the Dirichlet problem to obtain more accurate boundary data for the smaller box.

Once we have determined a discrete free space Green's function $g(i,j,k)$ we can compute the potential due to the screening charges $q(i,j,k)$ at points in the embedding region R. At any point p this potential is, of course, the discrete convolution of g with the charges:

$$\psi(i,j,k) = \sum_{i',j',k'} g(i-i', j-j', k-k')q(i',j',k'). \tag{5.1}$$

One very fast way of performing the calculation is by using an algorithm originally proposed by James, which is a modification of an algorithm initially popularized by Hockney [19]. In three dimensions Hockney's method requires twice the storage needed for the original mesh, and some sophisticated programming. Essentially, the method uses the fact that if one reflects the Green's function in each coordinate direction and convolves with the original charge one obtains the correct potential on the original mesh.

In the James algorithm the doubling procedure is used to calculate the free space potential due to the screening charges, but the doubling is only of the boundary values, and not the whole mesh. The operation count of the algorithm is $O(n^3 \log_2 n)$ where n is the number of mesh points in each direction in the embedding region, and the extra storage is minimal. In our calculations we first found the potential due to screening charges at points on ∂R by direct calculation using (5.1). Then we computed the potential inside R using a fast Poisson solver.

6. Operation counts and extensions

Once the discrete second or fourth order free space Green's function have been determined, the computational cost of the methods is essentially equal to twice the costs of inverting the the discrete Laplacians.

For example, if we are using the fourth order discretization method, computing the discrete Laplacian of ϕ_h has a cost $O(n^2)$ operations since there are $O(n^2)$ irregular mesh points. Using Fourier methods to invert the 19 point stencil to determine ϕ_h, requires $O(n^3 \log_2 n)$ operations (the constant is approximately 10). Finding the screening charges takes $O(n^3)$ operations and convolving them with the free space Green's function requires $O(n^3 \log n)$ operations. Subtracting the potentials, i.e. forming $U_h = \phi_h - \psi_h$ only requires $O(n^3)$ operations. Thus the total operation count is asymptotically twice the cost of the Fourier inversion methods, or $O(n^3 \log n)$, where the constant is approximately 20.

When we use the extrapolation method, determining the potential function ϕ_{1h} by the FACR algorithm has an operation count of $O(n^3 \log\log n)$, as does determining ϕ_{2h}, although since the coarser mesh has only 1/8th the number of points, the constant is more than eight times smaller there. Finding the screening charges takes $O(n^2)$ operations, while the operation counts for convolving the screening charges with the discrete second order free space Green's functions are $O(n^3 \log\log n)$. Forming the linear combination of the final potentials

$\widetilde{U}_{1h}$ and U_{2h} requires $O(n^3)$ operations. So in this case the total operation count is $O(n^3 \log\log n)$, which is smaller than the operation count for the fourth order discretization method.

We note that the methods we have presented allow us to obtain fourth order accurate approximations to other integrals in potential theory. For example, we can evaluate certain surface integrals and derivatives of the surface and volume integrals.

In order to evaluate surface integrals we can use the same basic method that we use to evaluate the volume integrals. In particular, we can use it to evaluate integrals of single layer density functions:

$$W^{\mathrm{s}}(x,y,z) = 1/4\pi \int\int_{\partial D} \rho(s,t)(1/r)\mathrm{d}S$$

and integrals of double layer density functions:

$$W^{\mathrm{d}}(x,y,z) = 1/4\pi \int\int_{\partial D} \mu(s,t)\frac{\partial}{\partial n_{\mathrm{s}}}(1/r)\mathrm{d}S.$$

As when we evaluate volume integrals, the problem of evaluating these integrals reduces to evaluating their Laplacians in the integration regions and outside, and evaluating the discontinuities in their derivatives at the boundary.

We first note that the Laplacians of both integrals vanish in the two regions.

To determine discontinuities in integrals of single layer density function we note that they are continuous in the tangential direction, and have a discontinuity equal to their density in the normal direction [38]. Similarly, to determine discontinuities in integrals of double layer density functions we use the facts that they are continuous in the normal direction and their discontinuity in the tangential derivative is equal to their density function. Once again these discontinuities determine the discontinuities in the derivatives of these integrals in any directions [31], and these are used to determine the discrete Laplacians at the irregular mesh points.

We now show how to evaluate derivatives, or a linear combination of the derivatives of a surface or volume integral.

To evaluate discontinuities in derivatives of integrals with differentiated kernels we use the fact that those integrals are derivatives of integrals with undifferentiated kernels. For example, suppose

$$\Omega(x,y,z) = \frac{1}{4\pi}\int\int_D\int \frac{\partial}{\partial x}\frac{1}{r(x,y,z,x',y',z')}f(x',y',z')\mathrm{d}V.$$

We note that $\Omega = U_x$ where

$$U(x,y,z) = \frac{1}{4\pi}\int\int_D\int \frac{1}{r(x,y,z,x',y',z')}f(x',y',z')\mathrm{d}V.$$

Since we know how to compute the discontinuities in the derivatives of U, we can, of course, compute the discontinuities in the derivatives of $\Omega = U_x$. As before, once we know the discontinuity terms we can use them to approximate the discrete Laplacian of Ω. Once we know the discrete Laplacian, we invert it to determine Ω.

Finally, we note that if one solves a boundary integral equation, one can solve Poisson problems with discontinuous but constant coefficients using the methods presented [31].

7. Numerical experiments

In this section we report on results of numerical experiments.

We tested our methods on problems where the regions of integration were unions of spheres or unions of ellipsoids. The computations were performed in double precision, and as mentioned above, once the discrete Green's functions were determined the running times were essentially equal to twice the time needed to apply a three-dimensional Poisson solver. That is, when we used the fourth order accurate stencil the running time was essentially twice the time needed to use Fourier methods to invert the fourth order discrete Laplacian on the embedding region, and when we used the extrapolation method it was essentially twice the time needed to apply the FACR algorithm on the embedding region.

When the integration regions were unions of spheres the integrals could be evaluated analytically, both inside and outside the region of integration. We could therefore determine errors and rates of convergence. In particular, we note that if the integration region D consists of a single sphere, $(x-c_x)^2+(y-c_y)^2+(z-c_z)^2=r_0^2$, and the inhomogeneous term is constant, $f=f_0$, then the value of the integral U is equal to $f_0\left(\frac{r^2}{6r_0^2}-\frac{1}{2}\right)$ at points inside the sphere, and $-\frac{f_0 r_0}{3r}$ at points outside where $r=\sqrt{(x-c_x)^2+(y-c_y)^2+(z-c_z)^2}$. If the inhomogeneous term is $f=20r^2$, the exact solution is $\frac{-3r^4+5r^2}{2}$ inside D, and $\frac{1}{r}$ outside D. When the regions of integration are unions of spheres then since integration is a linear functional, the values of the integral at a given point are the sums of the values of the integral over the individual spheres. When the regions of integration were unions of ellipsoids $\frac{(x-c_x)^2}{a^2}+\frac{(y-c_y)^2}{b^2}+\frac{(z-c_z)^2}{c^2}=1$, we used the solution on the finest mesh, 128 points in each direction, as the reference solution. That is we assumed that the solution computed on the 128 by 128 by 128 mesh was the exact solution and compared the others to it.

Both the spheres and ellipsoids were parametrized using Cartesian coordinates, i.e. we let $s=x$, $t=y$, so that $x(s,t)=x$, $y(s,t)=y$, and $z(s,\ t)=c_z+c\sqrt{(1-(x-c_x)^2/a^2-(y-c_y)^2/b^2)}$.

In Table 1a we give results of calculations using the fourth order accurate stencil to calculate the integral (2.1) for $f=-3$. The integration region D was the unit sphere centered at the origin, and the embedding region was the cube $[-1.51,1.51]^3$.

The numbers n in column 1 are the number of mesh points in each direction in the embedding cube, the numbers in the next column are the maximum relative errors, the numbers in column 4 are the L^2 norms of the relative errors, and the numbers in columns 3 and 5 specify the rate of convergence (i.e., the power of h reduction in the error) measured in the L^∞ norm and the L^2 norm, respectively.

In Table 1b we give results of using our extrapolation method to evaluate the same integral.

We see that the extrapolation method is slightly less accurate on this and other problems, but recall that the computation times are also slightly shorter. More precisely, since the number of operations needed to invert the 7 point discrete Laplacian in three dimensions on an n by n by n grid is approximately $5\,n^3\log\log n$, while the number required to invert the the 19 point Lapacian is $10\,n^3\log n$, the ratio of operation counts approaches $2\log n/\log\log n$. The difference is more significant the larger n is.

In Table 2 we give results of experiments where the integration regions were ellipsoids with semiaxes $a=1$, $b=0.6$ and $c=0.3$. The embedding region and inhomogeneous term were the same as in the previous example.

Next, we used our fourth order discretization method on a problem where the integration region consisted of two touching unit spheres and on a problem where the integration region consisted of two touching ellipsoids. The spheres were centered at $(-1,0,0)$ and $(1,0,0)$, and the ellipsoids were centered at the same points

Table 1a
Unit sphere, fourth order discretization

n	L^∞ error	Rate	L^2 error	Rate
16	0.522E − 03	3.68	0.276E − 03	3.94
32	0.408E − 04	3.81	0.180E − 04	3.96
64	0.290E − 05	3.99	0.115E − 05	4.01
128	0.183E − 06		0.713E − 07	

Table 1b
Unit sphere, extrapolation method

n	L^∞ error	Rate	L^2 error	Rate
16	0.165E − 02	3.57	0.115E − 02	3.75
32	0.138E − 03	3.80	0.851E − 04	3.94
64	0.994E − 05	4.00	0.554E − 05	4.02
128	0.621E − 06		0.341E − 06	

Table 2a
Ellipsoid, fourth order discretization

n	L^∞ error	Rate	L^2 error	Rate
16	0.694E − 03	3.97	0.372E − 03	4.00
32	0.443E − 04	3.91	0.233E − 04	4.00
64	0.294E − 05		0.146E − 05	

Table 2b
Ellipsoid, extrapolation method

n	L^∞ error	Rate	L^2 error	Rate
16	0.371E − 02	4.01	0.175E − 02	4.02
32	0.231E − 03	3.94	0.108E − 03	3.96
64	0.150E − 04		0.696E − 05	

and had semiaxes $a = 1$, $b = 0.5$ and $c = 0.25$. In each sphere and ellipsoid the inhomogeneous term f was equal to -3. In both cases the embedding region was the cube $[-2.51, 2.51]^3$. Results are given in Tables 3a and 3b.

In Table 4 we give results of using our extrapolation method to compute integrals over the same regions as in the previous example. The integration and embedding regions as well as the inhomogeneous term were also the same as in Table 3. The errors and convergence rates are for the L^2 norm.

Results in Table 5 are for calculating the x derivative of the integral with inhomogeneous term $f = 3$ on the unit sphere centered at the origin and on the ellipsoid with semiaxes $a = 1$, $b = 0.4$ and $c = 0.2$ using the extrapolation method. The embedding region was the cube $[-4.1, 4.1]^3$. See Tables 6a and 6b.

Table 3a
Two spheres, fourth order discretization

n	L^∞ error	Rate	L^2 error	Rate
16	0.387E − 02	3.96	0.813E − 03	4.00
32	0.249E − 03	3.90	0.508E − 04	3.99
64	0.166E − 04	3.96	0.321E − 05	4.01
128	0.107E − 05		0.199E − 06	

Table 3b
Two ellipsoids, fourth order discretization

n	L^∞ error	Rate	L^2 error	Rate
16	0.493E − 02	3.95	0.159E − 02	3.87
32	0.319E − 03	3.95	0.109E − 03	4.00
64	0.206E − 04		0.682E − 05	

Table 4
Extrapolation method

n	Two spheres		Two ellipsoids	
	L^2 error	Rate	L^2 error	Rate
16	0.635E − 02	3.85	0.901E − 02	3.95
32	0.441E − 03	3.86	0.584E − 03	4.02
64	0.303E − 04	4.00	0.358E − 04	
128	0.189E − 05			

Table 5a
Sphere, x derivatives, extrapolation method

n	L^∞ error	Rate	L^2 error	Rate
16	0.774E − 02	3.74	0.676E − 02	3.73
32	0.580E − 03	3.65	0.510E − 03	3.97
64	0.461E − 04	4.03	0.325E − 04	4.00
128	0.282E − 05		0.203E − 05	

Table 5b
Ellipsoid, x derivatives, extrapolation method

n	L^∞ error	Rate	L^2 error	Rate
16	0.135E − 01	3.87	0.983E − 02	3.93
32	0.926E − 03	3.91	0.642E − 03	3.94
64	0.618E − 04		0.418E − 04	

Table 6a
Sphere, $f = r^2$, extrapolation method

n	L^∞ error	Rate	L^2 error	Rate
16	0.950E − 03	3.91	0.571E − 03	3.96
32	0.631E − 04	3.93	0.366E − 04	3.94
64	0.413E − 05	4.01	0.241E − 05	4.00
128	0.257E − 06		0.150E − 06	

Table 6b
Ellipsoid, $f = r^2$, extrapolation method

n	L^∞ error	Rate	L^2 error	Rate
16	0.139E − 02	3.95	0.899E − 03	3.89
32	0.897E − 04	3.97	0.605E − 04	4.01
64	0.574E − 05		0.376E − 05	

In our next experiments the integration regions were the same as in the previous example, and the integrals were computed using the extrapolation method. This time the inhomogeneous term was $f = 20r^2$, and the embedding region was $[-3.5, 3.5]^3$.

In Table 7 we present results of experiments using our fourth order discretization method where the integration regions consisted of four spheres of radius 0.8 (first two columns) or four ellipsoids with semiaxes $a = 0.8$, $b = 0.6$ and $c = 0.4$ second two columns). The centers of the spheres and ellipsoids were $(-1.25, 0, 0)$, $(1.25, 0, 0)$, $(0, -1.250)$, and $(0, 1.25, 0)$, the inhomogeneous terms were set to -3 on all the regions, and the embedding regions were the cube $[-2.61, 2.61]^3$.

Table 7
Fourth order discretization

n	Four spheres		Four ellipsoids	
	L^∞ error	Rate	L^∞ error	Rate
16	0.198E − 01	3.94	0.317E − 01	3.88
32	0.129E − 02	3.98	0.215E − 02	3.96
64	0.818E − 04	4.00	0.138E − 03	
128	0.511E − 05			

8. Conclusions

We have presented two fourth order accurate methods for evaluating volume integrals in potential theory on general three-dimensional regions in free space. One of the methods uses a compact, high order stencil, and the other is an extrapolation method. Both methods use standard Poisson solvers on a larger region in which the irregular region is embedded. In addition they require the use of a discrete free space Green's function. We have performed numerical experiments on a variety of exterior regions that demonstrate that our proposed methods are indeed fourth order accurate.

References

[1] B. Alpert, G. Beylkin, R. Coifman, V. Rokhlin, Wavelets for the fast solution of second kind integral equations, SIAM J. Sci. Comp. 14 (1993) 1, 159.
[2] A. Armstrong, C. Collie, J. Simpkin, C. Trowbridge, The solution of 3D magnetostatic problems using scalar potentials, Rutherford Laboratory, RL-78-078, September, 1978.
[3] T. Beale, A. Lai, On the accuracy of finite difference methods for elliptic problems with interfaces, manuscript.
[4] G. Biros, L. Ying, D. Zorin, The embedded boundary integral method for the incompressible Navier Stokes equations, in: Proceedings of the International Association for Boundary Element Methods, 2002 Symposium, CDROM, University of Texas at Austin, Austin TX, May 28–30, 2002.
[5] G. Biros, L. Ying, D. Zorin, A fast solver for the Stokes equations with distributed fores in complex geometries, J. Comput. Phys. 194 (1) (2004) 317.
[6] C. Brebbia, The Boundary Element Method For Engineers, John Wiley and Sons Inc., New York, 1978.
[7] O. Buneman, A compact noniterative Poisson solverRep. SUIPR-294, Inst. Plasma Research, Stanford University, Stanford, CA, 1969.
[8] O. Buneman, Analytic inversion of the five point operator, JCP 8 (1971) 500–505.
[9] R. Burkhart, Asymptotic expansion of the free space Greens function for the discrete Poisson equation, SIAM J. Sci. Comp. 18 (1997) 1142.
[10] B. Buzbee, F. Dorr, J. George, G. Golub, The direct solution of the discrete Poisson equation on irregular domains, SIAM J. Numer. Anal. 8 (1971) 722.
[11] F. Etheridge, L. Greengard, A new fast-multipole accelerated Poisson solver in two dimensions, SIAM J. Sci. Comp. 23 (3) (2001) 741.
[12] F. Gibou, R. Fedkiw, A fourth order accurate discretization for the Laplace and heat equations on arbitrary domains with applications to the Stefan problem, J. Comput. Phys. 171 (2001) 205.
[13] L. Fauci, C. Peskin, A computational model of aquatic animal locomotion, J. Comput. Phys. 17 (1988) 85.
[14] A. Greenbaum, L. Greengard, A. Mayo, The rapid numerical solution of the biharmonic equation, Physica D 60 (1992) 216.
[15] A. Greenbaum, A. Mayo, Rapid parallel evaluation of integrals in potential theory on general three-dimensional regions, J. Comput. Phys. 145 (1998) 731.
[16] L. Greengard, J.Y. Lee, A direct adaptive Poisson solver of arbitrary order accuracy, J. Comput. Phys. 125 (1996) 415.
[17] L. Greengard, V. Rokhlin, A new version of the fast multipole method for the Laplace equation in three dimensions, Acta Numerica (1997) 229.
[18] L. Greengard, M.C. Kropinski, A. Mayo, Integral equation methods for Stokes flow and isotropic elasticity in the plane, J. Comput. Phys. 125 (1996) 403.
[19] R. Hockney, A fast direct solution of Poisson's equation using Fourier analysis, J. Assoc. Comput. Mach. 12 (1965) 95–133.
[20] R. HockneyMethods in Computational Physics, vol. 9, Academic Press, New York, 1970, pp. 135–211.
[21] R. Hockney, J. Eastwood, Computer Simulation Using Particles, McGraw Hill, 1985.
[22] R. James, The solution of Poissons equation for for isolated source distributions, J. Comput. Phys. 25 (71) (1977) 1534.
[23] H. Johansen, P. Colella, A Cartesian grid embedded boundary method for Poisson's equation on irregular domains, J. Comput. Phys. 147 (1998) 60.
[24] O. Kellogg, Foundations of Potential Theory, Dover, New York, 1953.
[25] M. Lean, D. Bloomberg, Nonlinear boundary element method for two dimensional magnetostatics, J. Appl. Phys. 55 (6) (1984) 2195.
[26] R. Leveque, Z. Li, The immersed interface method for elliptic equations with discontinuous coefficients and singular sources, SIAM J. Numer. Anal. 31 (1994) 1019.
[27] Z. Li, M. Lai, The immersed interface method for the Navier Stokes equations with singular forces, J. Comput. Phys. 171 (2001) 822.
[28] Z. Li, A. Mayo, ADI Methods for heat equations with discontinuities along an arbitrary interface, Proc. Symp. Appl. Math. (PSAPM), AMS 48 (1994) 311.
[29] D. Lindholm, Three dimensional magnetostatic fields from point matched integral equations with linearly varying scalar sources, IEEE Trans. Magn. 20 (5) (1984) 143.
[30] A. McKenney, L. Greengard, A. Mayo, A fast Poisson solver for complex geometries, J. Comput. Phys 118 (1995) 348.
[31] A. Mayo, A. Greenbaum, Fast parallel solution of Poisson's and the biharmonic equations on irregular regions, SIAM J. Sci. Stat. Comput. 13 (1) (1992) 1.

[32] A. Mayo, Rapid methods for the conformal mapping of multiconnected regions, Journal of Computational and Applied Mathematics 14 (1986) 143.
[33] A. Mayo, The fast solution of Poisson's and the biharmonic equations on irregular regions, SIAM J. Numer. Anal. 21 (2) (1984) 285.
[34] A. Mayo, The rapid evaluation of volume integrals of potential theory on general regions, J. Comput. Phys. 100 (2) (1992) 236.
[35] A. Mayo, Rapid, fourth order accurate evaluation of particular solutions of the biharmonic equation on general regionsContemp. Math. COMN 323, AMS Publications, Providence, 2003, p. 233.
[36] A. Mayo, Rapid, fourth order accurate solution of the steady Navier Stokes equations on general regions, Dyn. Contin. Discrete Impulsive Syst., to appear 2005.
[37] A. Mayo, Rapid fourth order accurate methods of the solution of the Stokes equations in the presence of an immersed boundary, IBM Research Report, RC 19603, 1994. IBM Research Report.
[38] S.G. Mikhlin, Integral Equations, Pergamon Press, New York, 1957.
[39] C. Peskin, D. McQueen, A three dimensional computational method for blood flow in the heart i. Immersed elastic fibers in a viscous incompressible fluid, J. Comput. Phys 81 (1989) 372.
[40] C. Pozrikidis, Boundary Integral and Singularity Methods for Linearized Viscous Flow, Cambridge University Press, 1992.
[41] W. Proskurowski, O. Widlund, On the numerical solution of Helmholz's equation by the capacitance matrix method, Math. Comput. 30 (135) (1976) 433.
[42] V. Rokhlin, Rapid solution of integral equations of classical potential theory, J. Comput. Phys. 60 (1985) 187.
[43] V. Rokhlin, Rapid solution of integral equations of scattering in two dimensions, J. Comput. Phys. 106 (1993) 355.
[44] J. Ruppert, R. Seidel, On the difficulty of triangulating three dimensional nonconvex polyhedra, Discrete Comput. Geom. 7 (4) (1992).
[45] K. Von Hagenow, K. Lackner, in: Proceedings of the 7th Conference on Numerical Simulation of Plasma, New York, 1975.
[46] Y.Z. Zhou, S. Zhao, M. Feig, G.W. Wei, High order matched interface and boundary method for elliptic equations with discontinuous coefficients and singular sources, J. Comput. Phys. 212 (2006) 1.